Bulk Signatures of Pressure-Induced Band Inversion and Topological Phase Transitions in $Pb_{1-x}Sn_xSe$

Xiaoxiang Xi,[1] Xu-Gang He,[2,3] Fen Guan,[3] Zhenxian Liu,[4] R. D. Zhong,[2] J. A. Schneeloch,[2] T. S. Liu,[2,5] G. D. Gu,[2] X. Du,[3] Z. Chen,[6] X. G. Hong,[6] Wei Ku,[2] and G. L. Carr[1]

[1]*Photon Sciences, Brookhaven National Laboratory, Upton, New York 11973, USA*
[2]*Condensed Matter Physics and Materials Science Department, Brookhaven National Laboratory, Upton, New York 11973, USA*
[3]*Department of Physics and Astronomy, Stony Brook University, Stony Brook, New York 11794, USA*
[4]*Geophysical Laboratory, Carnegie Institution of Washington, Washington DC 20015, USA*
[5]*School of Chemical Engineering and Environment, North University of China, Taiyuan 030051, China*
[6]*Department of Geosciences, Stony Brook University, Stony Brook, New York 11794, USA*
(Received 6 June 2014; published 27 August 2014; corrected 13 October 2014)

The characteristics of topological insulators are manifested in both their surface and bulk properties, but the latter remain to be explored. Here we report bulk signatures of pressure-induced band inversion and topological phase transitions in $Pb_{1-x}Sn_xSe$ ($x = 0.00$, 0.15, and 0.23). The results of infrared measurements as a function of pressure indicate the closing and the reopening of the band gap as well as a maximum in the free carrier spectral weight. The enhanced density of states near the band gap in the topological phase gives rise to a steep interband absorption edge. The change of density of states also yields a maximum in the pressure dependence of the Fermi level. Thus, our conclusive results provide a consistent picture of pressure-induced topological phase transitions and highlight the bulk origin of the novel properties in topological insulators.

Topological insulators (TIs) represent a new phase of matter that completely defies Landau's spontaneous symmetry breaking framework [1,2]. Their insulating bulk is topologically nonequivalent to the vacuum, giving rise to metallic surface states. Such exotic properties come with a conundrum: The topological invariants characterizing the topological property are defined using the bulk electronic wave functions, but nevertheless remain elusive to bulk experimental probes. To date, the proof of the existence of TIs is based on the detection of the metallic surface states [1,2]. Exploiting the surface spin texture, spin-resolved angle-resolved photoemission spectroscopy provides the only measure of the topological invariants in three-dimensional (3D) TIs [3,4]. Despite the great amount of research activity in this field, the bulk properties of TIs that are intimately tied to the nontrivial topology are mostly unexplored. Establishing the bulk properties can complete our understanding of TIs and facilitate their identification.

An effective approach for establishing the bulk signatures of TIs is to follow the evolution of characteristic features, starting from the trivial insulating state through the topological phase transition (TPT) and into the TI phase. Applying pressure offers a particularly attractive method for controllably driving a material through such a transition. Generally, a hallmark of a TPT in a noninteracting system is band inversion [5]: The bulk band gap closes at the phase transition and reopens afterward, inverting the characters of the bottom conduction band and top valence band. Although the resulting change in the bulk band structure is expected to be dramatic, detecting and understanding the associated experimental signatures are surprisingly challenging. For example, angle-resolved photoemission spectroscopy is not compatible with pressure tuning nor is it sensitive to the bulk. Previously, two groups [6,7] reported investigations for a pressure-induced TPT in BiTeI [8], but reached different and actually contradictory conclusions. In one case [6], an observed maximum in the free carrier spectral weight was interpreted as strong evidence for a TPT. In the other [7], a monotonic redshift of the interband absorption edge was interpreted to indicate the absence of such a transition. Obviously, resolving this contradiction is necessary for our understanding of TIs to move forward.

Here we clarify this current controversy by demonstrating bulk signatures of a pressure-induced band inversion and thus a TPT in $Pb_{1-x}Sn_xSe$ ($x = 0.00$, 0.15, and 0.23). A maximum in the free carrier spectral weight is reconfirmed in this system and is possibly a generic feature of pressure-induced TPTs when bulk free carriers are present. The absorption edge initially redshifts and then blueshifts under pressure, but only when its overlap with the intraband transition is suppressed. Extra evidence for the TPT is uncovered, including a steeper absorption edge in the topological phase compared to the trivial phase and a maximum in the pressure dependence of the Fermi level. The TPTs in $Pb_{1-x}Sn_xSe$ imply the creation of 3D Dirac semimetals at the critical pressure, serving as a route for pursuing Weyl semimetals [9]. The robust bulk signatures

of TPTs identified here are expected to be useful for exploring a variety of candidate pressure-induced TIs [10–12] and even topological materials with electronic correlation [13,14].

Lead chalcogenides are candidate topological crystalline insulators (TCIs) under pressure [15], with the role of time-reversal symmetry in TIs replaced by crystal symmetries [16]. Similar to TIs, TCIs' nontrivial band topology is associated with an inverted band structure, shown in SnTe [17,18], $Pb_{0.4}Sn_{0.6}Te$ [19], and $Pb_{0.77}Sn_{0.23}Se$ below 100 K [20]. These narrow-gap semiconductors crystallize in the rocksalt structure and share simple band structures ideal for investigating bulk characteristic of TPTs. At ambient condition, PbX (X = S, Se, or Te) has a direct band gap at the L point of the Brillouin zone, with the L_6^- (L_6^+) character for the bottom conduction band (top valence band) [15]. Band inversion is known to be induced in $Pb_{1-x}Sn_xX$ (X = Se and Te) by doping [21–23] or, in the series of Pb-rich alloys, by cooling [22,23], although the connection to band topology was only recently recognized [15,17]. Pressure-induced band inversion in PbSe and PbTe has been proposed on theoretical grounds [24], especially in the context of TPTs [15,17], but experimentally it has not been firmly established [25,26].

In this work, we present a systematic infrared study of pressure-induced band inversion in $Pb_{1-x}Sn_xSe$. Samples with nominal $x = 0.00$, 0.15, and 0.23 were synthesized by a modified floating zone method. Hall effect measurements determined a hole density of roughly 10^{18} cm^{-3} for PbSe at room temperature. High-pressure experiments were performed using diamond anvil cells at Beamline U2A of National Synchrotron Light Source, Brookhaven National Laboratory. Samples in the form of thin flakes (≤ 5 μm) were measured in transmission, while thicker (> 10 μm) pieces were measured in reflection. Details of the measurement procedures are described elsewhere [6].

For comparison with the experiment, an *ab initio* method based on the WIEN2K package [27] was used to simulate the pressure effects on PbSe. We combined the local spin density approximation and spin-orbit coupling for the self-consistent field calculations, adjusting only the lattice parameter a to mimic pressure effects. The mesh was set to $46 \times 46 \times 46k$ points and $R_{MT} \times K_{MAX} = 7$, where R_{MT} is the smallest muffin tin radius and K_{MAX} the plane wave cutoff. The effect of doping was considered in the self-consistent calculation according to the experimental hole density. While the calculation does not yield the exact lattice parameter at which the TPT occurs, we found the results to be in qualitative agreement with our experimental observations.

Lead chalcogenides exhibit structural phase transitions under pressure [28]. We determined that, at room temperature, $Pb_{1-x}Sn_xSe$ maintains the ambient-pressure structure up to 5.1, 4.0, and 2.9 GPa for $x = 0.00$, 0.15, and 0.23, respectively [29]. In the following, we focus on the

ambient-pressure structure and investigate pressure-induced TPTs.

We began by revealing a maximum in the pressure-dependence of the bulk free carrier spectral weight. In the same manner as for BiTeI [6], this serves as a signature of band inversion. Though the free carrier response of the bulk has made analysis of the surface behavior challenging, it actually provides a sensitive and convenient probe of band inversion and thus TPTs. For doped semiconductors with simple bands, the low-frequency dielectric function for intraband transitions can be described by $\varepsilon(\omega) = \varepsilon_\infty - \omega_p^2/(\omega^2 + i\omega\gamma)$, where ω is the photon frequency, ε_∞ the high-energy dielectric constant, $\omega_p^2/8$ the Drude spectral weight (ω_p the bare plasma frequency), and γ the electronic scattering rate. The Drude weight $\omega_p^2/8$ connects with the band dispersion through the Fermi velocity v_F, $\omega_p \propto v_F$ because ω_p^2 (in general as a tensor) for a single band is given by [29]

$$\omega_{p,\alpha\beta}^2 = \frac{\hbar^2 e^2}{\pi} \int d\mathbf{k}\, v_\alpha(\mathbf{k}) v_\beta(\mathbf{k}) \delta(E(\mathbf{k}) - E_F),$$

where $\mathbf{k}$ is the crystal momentum, $E(\mathbf{k})$ the band dispersion, $v_\alpha(\mathbf{k}) = [\partial E(\mathbf{k})/\partial k_\alpha]/\hbar$ the αth component of the Bloch electron mean velocity, and E_F the Fermi energy. The measured reflectance has a minimum near the zero crossing in the real part of $\varepsilon(\omega)$, called the plasma minimum, located at $\omega \sim \omega_p/\sqrt{\varepsilon_\infty}$ [32]. The plasma minimum is universally observed in $Pb_{1-x}Sn_xSe$ for $x = 0.00$, 0.15, and 0.23 (see Fig. 2). Upon increasing pressure, it initially blueshifts and then redshifts, indicated by the dashed lines in Fig. 2. Since the phase space for intraband transitions reaches a minimum at the gap-closing pressure and ε_∞ increases monotonically under pressure [29], the maximum in $\omega_p/\sqrt{\varepsilon_\infty}$ must be attributed to v_F going through a maximum near the critical pressure of the TPT [Fig. 1(d)]. This allows us to estimate the critical pressure to be 2.2, 0.9, and 0.7 GPa for $x = 0.00$, 0.15, and 0.23, respectively. The lowering of the critical pressure with increasing x is due to the systematic doping-induced suppression of the band gap [22,23]. The expression for $\varepsilon(\omega)$ provides excellent fits to our data, exemplified for $Pb_{0.77}Sn_{0.23}Se$ in Fig. 2(d) and quantifying the maximum in the pressure dependence of ω_p (Fig. 2(e) and Ref. [29]). Such a maximum was also observed in BiTeI [6,7] and is likely generic in pressure-induced TPTs when a significant carrier density exists.

Having established the TPTs, we now turn to the interband transitions to address the controversy over the absorption edge [6,7]. Figure 3(a) shows the absorbance [defined as $-\log(\text{transmittance})$] of PbSe at 298 K for pressures up to ~5.1 GPa, at which point a structural phase transition occurs [35]. To assist the discussion, we roughly define three photon energy regions, illustrated in Fig. 3(a). Region I is dominated by the intraband transition, but is outside the spectral range for the instrument used in the
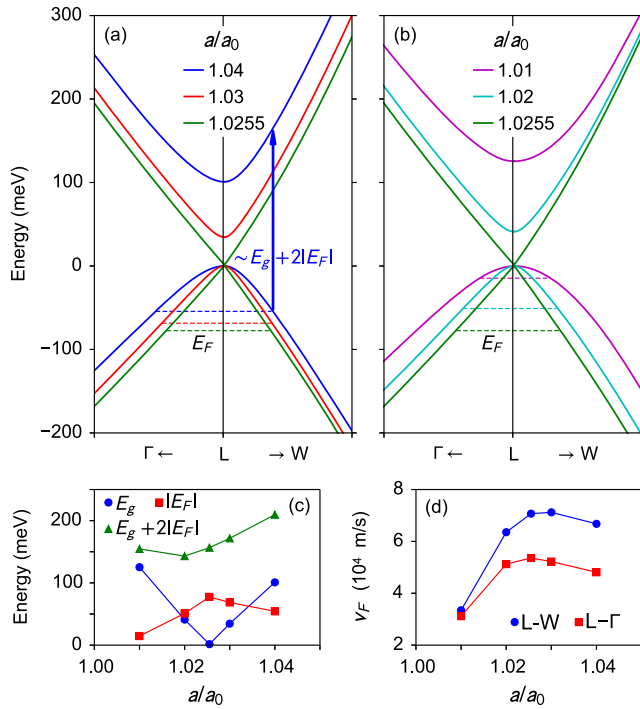
FIG. 1 (color online).　(a,b) Electronic band structure of PbSe at various lattice parameter ratio a/a_0 along the L-Γ and L-W directions of the Brillouin zone. a_0 is the experimental lattice constant in the zero temperature limit and at ambient pressure [33]. The TPT occurs at $a/a_0 \approx 1.0255$. The dashed lines indicate the Fermi level E_F for a hole density of $N = 10^{18}$ cm^{-3}. (c) The direct band gap E_g at the L point, absolute value of the Fermi level $|E_F|$ relative to the top valence band, and $E_g + 2|E_F|$ [roughly the energy threshold for direct interband transitions in the presence of free carriers, as indicated by the arrow in (a)] as a function of a/a_0. (d) Fermi velocity v_F along the L-Γ and L-W directions as a function of a/a_0 for $N = 10^{18}$ cm^{-3}.

measurement. Region III hosts the majority of the absorption edge, defined as the steep rising part due to the onset of interband transitions and indicated by the arrow in Fig. 3(a), which is expected to redshift and then blueshift across the TPT. The absorption edge shown in Region III of Fig. 3(a) redshifts monotonically under pressure, indicating band gap closing, but not reopening. Above 1.3 GPa, the initial rising part of the absorption edge which determines the band gap moves into Regions II and I, overlapping significantly with the intraband transition.

Close inspection of Region II in Fig. 3(a) reveals band gap reopening. Despite of the overlap with the conspicuous tail of the intraband transition, the interband absorption edge in Region II shows a clear change of slope: It becomes steeper as the pressure is increased to 5.1 GPa, possibly due to the band gap reopening. For a more conclusive observation of the band gap reopening, we cooled the sample to 70 K in order to reduce the electronic scattering rate γ so that the intraband transition peak became narrower and overlapped less with the interband absorption edge. As shown in Fig. 3(b), the absorption edge systematically tilts

toward higher photon energy from 2.4 to 4.2 GPa, suggesting that the band gap monotonically increases. The TPT at 70 K most likely occurs below 2.2 GPa (the critical pressure at room temperature) because cooling the sample reduces the lattice parameter a [33]. Finally, a structural phase transition occurs at 4.5 GPa (at 70 K), causing a dramatic overall decrease of absorbance. Pressure-induced band gap closing and reopening were also observed in PbTe at low temperature [29].

The above discussion illustrates the complexity of analyzing the interband absorption edge to identify gap closure and band inversion at a TPT. Considering the apparent monotonic increase of spectral weight in Region III [see Fig. 3(a)] as a function of pressure, one might conclude that a TPT had not occurred. But the key signature of gap closure is obscured by overlap with the intraband absorption, as well as by thermal broadening. This can be circumvented by cooling the material, revealing both the redshift and then blueshift of the absorption edge as the band gap closes and then reopens. The situation for BiTeI is even more complicated due to the Rashba splitting and the additional optical transitions among the split subbands [6,7]. Cooling does not alleviate this complication. Thus, inferring how the band gap changes in that and similar materials from measurements to sense the absorption edge is not practical.

In the rest of this Letter, we present two more signatures of pressure-induced TPTs in PbSe, namely a steeper absorption edge in the topological phase and a maximum in the pressure dependence of the Fermi level.

The absorption edge becomes steeper after the TPT, distinguishing the topological phase from the trivial phase. Such behavior is clearly observed in Fig. 3(b) and confirmed by the calculated optical conductivity shown in Fig. 3(c). The results emphasize the hybridization nature of the band gap in a TI (or TCI) as illustrated in Fig. 3(d), qualitatively different from that in a trivial insulator. As demonstrated by the evolution of the band structure across a TPT close to the direct band gap, shown in Figs. 1(a) and 1(b), before the TPT, pressure suppresses the band gap and transforms the band dispersion from a near-parabolic shape to almost linear. After the TPT, the band dispersion briefly recovers the near-parabolic shape and then flattens. [At even higher pressure, it develops a Mexican-hat feature [29] similar to that illustrated in Fig. 3(d).] The flat band makes the joint density of states just above the band gap much greater than that of an ordinary insulator with the same band gap size, yielding a steeper absorption edge. It also gives rise to van Hove singularities that differ from the typical ones [36], shown as peaks in the optical conductivity for $a/a_0 = 1.01$ and 1.00 in Fig. 3(c).

Such a peak feature was previously observed (although unexplained) in the Bi$_2$Te$_2$Se TI material with low free carrier density [37,38], but is absent in our infrared absorbance data shown in Figs. 3(a) and 3(b), possibly for two reasons. First, the peak only appears deep in the
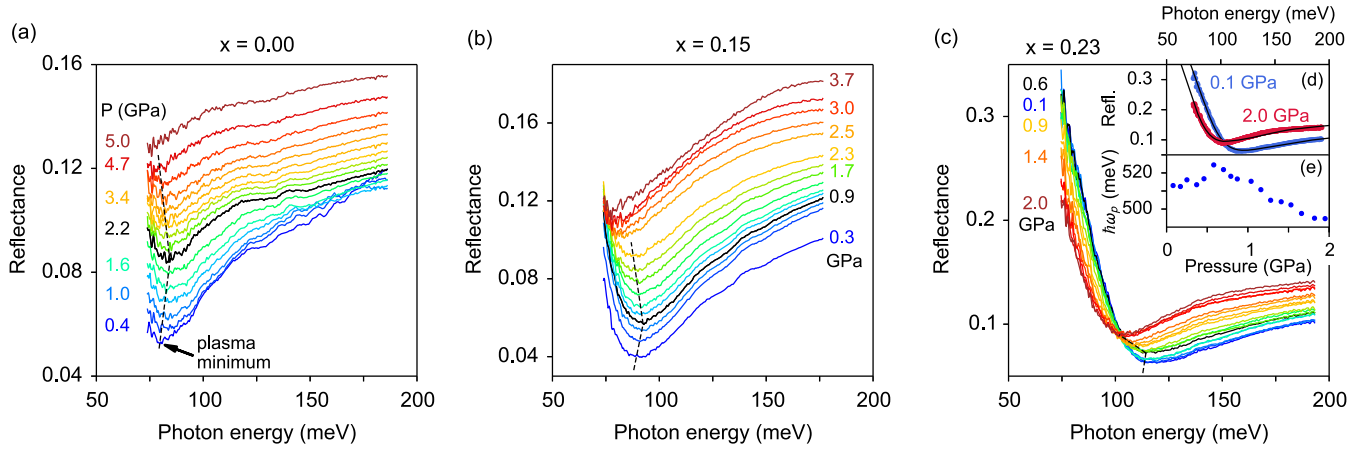
FIG. 2 (color online).   (a–c) Pressure-dependent midinfrared reflectance of $Pb_{1-x}Sn_xSe$ measured at the diamond-sample interface and at room temperature [34]. The dashed lines are guides to the eye for the shift of the plasma minimum. (d) Example fits (solid lines) to the experimental data of $x = 0.23$ (dots). (e) Pressure dependence of ω_p extracted from the fit.

topological phase, which requires a high pressure that in reality causes a structural phase transition. Second, the Burstein-Moss effect (see the next paragraph) in our sample precludes optical transitions connecting the states near the top valence band and the bottom conduction band and thus the observation of van Hove singularities. The dashed line in Fig. 3(c) demonstrates that holes with a density of 10^{18} cm^{-3} completely smears the sharp peak.

Finally, our calculation shows a maximum in the pressure-dependence of the Fermi level $|E_F|$ at the gap-closing pressure [Fig. 1(c)], which can be measured from Shubnikov–de Haas oscillations [39] to support the TPT. This maximum in $|E_F|$ happens because the density of states near the top valence band diminishes as the band dispersion becomes linear [29], pushing the Fermi level away from the top valence band to conserve the phase space for the holes. This effect also manifests in the infrared spectra, although E_F cannot be easily determined from

them. When free carriers are present, the band gap associated with the absorption edge is not the true band gap in the electronic band structure. As illustrated in Fig. 1(a), the holes shift the Fermi level to below the top valence band, making the energy threshold for direct interband transitions approximately $E_g + 2|E_F|$, known as the Burstein-Moss effect. The absorption edge character-izes $E_g + 2|E_F|$ instead of E_g. The combined pressure effects on E_g and E_F retain a minimum in $E_g + 2|E_F|$, but the corresponding pressure could be different from the critical pressure for band gap closing, shown in Fig. 1(c). Moreover, the absorption edge never redshifts to zero photon energy even when $E_g = 0$. The Burstein-Moss effect adds further difficulty to the identification of TPTs using the absorption edge.

To summarize, we have established bulk signatures of pressure-induced band inversion and thus TPTs in $Pb_{1-x}Sn_xSe$ ($x = 0.00$, 0.15, and 0.23). Infrared reflectance
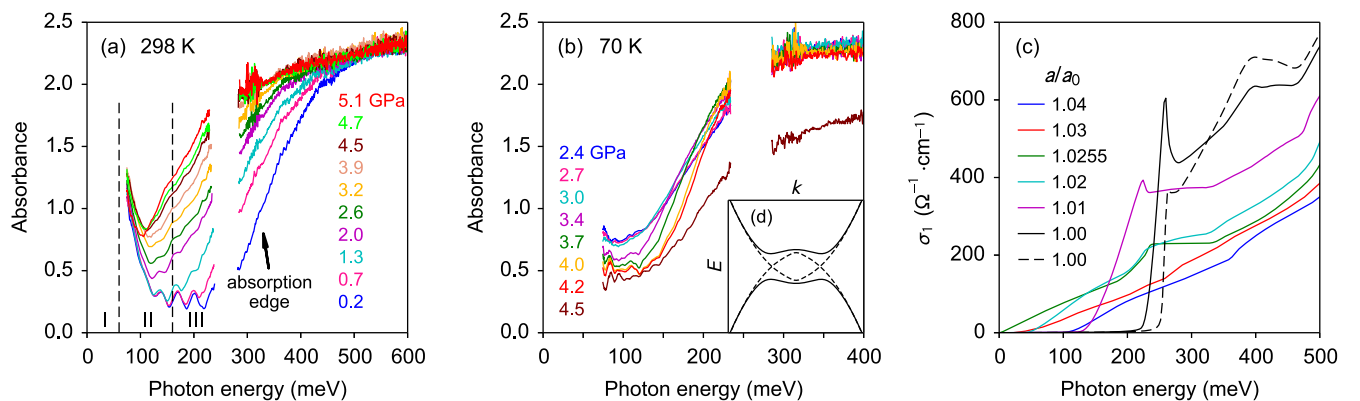

FIG. 3 (color online).   Pressure-dependent midinfrared absorbance of PbSe measured at (a) 298 K and (b) 70 K [34]. Data in the blank region between 200–300 meV are not shown because of unreliability caused by diamond absorption. (c) Real part of the interband optical conductivity σ_1 of intrinsic PbSe at various a/a_0 from first-principles calculations. The dashed line shows the result including holes with a density of 10^{18} cm^{-3}. (d) [inset to (b)] A diagram illustrating hybridization opens up a band gap (in the bands shown as solid lines) when the conduction band and valence band cross (dashed lines).

shows a maximum in the bulk free carrier spectral weight near the gap-closing pressure. The interband absorption edge tracks the change of the band gap across the TPT; however, the free carriers complicate the picture due to the overlap with the intraband transition and the shift of the Fermi level. The absorption edge becomes steeper in the topological phase due to the hybridization nature of the band gap in TIs. A maximum in the pressure dependence of the Fermi level is also expected. These robust bulk features complement the surface-sensitive techniques and serve as a starting point to investigate TPTs in more complicated systems.

[1] M. Z. Hasan and C. L. Kane, Rev. Mod. Phys. **82**, 3045 (2010).

[2] X. L. Qi and S. C. Zhang, Rev. Mod. Phys. **83**, 1057 (2011).

[3] D. Hsieh, Y. Xia, L. Wray, D. Qian, A. Pal, J. H. Dil, J. Osterwalder, F. Meier, G. Bihlmayer, C. L. Kane, Y. S. Hor, R. J. Cava, and M. Z. Hasan, Science **323**, 919 (2009).

[4] S.-Y. Xu, Y. Xia, L. A. Wray, S. Jia, F. Meier, J. H. Dil, J. Osterwalder, B. Slomski, A. Bansil, H. Lin, R. J. Cava, and M. Z. Hasan, Science **332**, 560 (2011).

[5] H. Zhang, C.-X. Liu, X.-L. Qi, X. Dai, Z. Fang, and S.-C. Zhang, Nat. Phys. **5**, 438 (2009).

[6] X. Xi, C. Ma, Z. Liu, Z. Chen, W. Ku, H. Berger, C. Martin, D. B. Tanner, and G. L. Carr, Phys. Rev. Lett. **111**, 155701 (2013).

[7] M. K. Tran, J. Levallois, P. Lerch, J. Teyssier, A. B. Kuzmenko, G. Autés, O. V. Yazyev, A. Ubaldini, E. Giannini, D. van der Marel, and A. Akrap, Phys. Rev. Lett. **112**, 047402 (2014).

[8] M. S. Bahramy, B.-J. Yang, R. Arita, and N. Nagaosa, Nat. Commun. **3**, 679 (2012).

[9] E. V. Gorbar, V. A. Miransky, and I. A. Shovkovy, Phys. Rev. B **89**, 085126 (2014).

[10] S. Chadov, X. L. Qi, J. Kübler, G. H. Fecher, C. Felser, and S. C. Zhang, Nat. Mater. **9**, 541 (2010).

[11] B. Sa, J. Zhou, Z. Song, Z. Sun, and R. Ahuja, Phys. Rev. B **84**, 085130 (2011).

[12] W. Li, X.-Y. Wei, J.-X. Zhu, C. S. Ting, and Y. Chen, Phys. Rev. B **89**, 035101 (2014).

[13] B.-J. Yang and Y. B. Kim, Phys. Rev. B **82**, 085111 (2010).

[14] C. H. Kim, H. S. Kim, H. Jeong, H. Jin, and J. Yu, Phys. Rev. Lett. **108**, 106401 (2012).

[15] P. Barone, T. Rauch, D. Di Sante, J. Henk, I. Mertig, and S. Picozzi, Phys. Rev. B **88**, 045207 (2013).

[16] L. Fu, Phys. Rev. Lett. **106**, 106802 (2011).

[17] T. H. Hsieh, H. Lin, J. W. Liu, W. H. Duan, A. Bansil, and L. Fu, Nat. Commun. **3**, 982 (2012).

[18] Y. Tanaka, Z. Ren, T. Sato, K. Nakayama, S. Souma, T. Takahashi, K. Segawa, and Y. Ando, Nat. Phys. **8**, 800 (2012).

[19] S.-Y. Xu, C. Liu, N. Alidoust, M. Neupane, D. Qian, I. Belopolski, J. D. Denlinger, Y. J. Wang, H. Lin, L. A. Wray, G. Landolt, B. Slomski, J. H. Dil, A. Marcinkova, E. Morosan, Q. Gibson, R. Sankar, F. C. Chou, R. J. Cava, A. Bansil, and M. Z. Hasan, Nat. Commun. **3**, 1192 (2012).

[20] P. Dziawa, B. J. Kowalski, K. Dybko, R. Buczko, A. Szczerbakow, M. Szot, E. Łusakowska, T. Balasubramanian, B. M. Wojek, M. H. Berntsen, O. Tjernberg, and T. Story, Nat. Mater. **11**, 1023 (2012).

[21] J. O. Dimmock, I. Melngailis, and A. J. Strauss, Phys. Rev. Lett. **16**, 1193 (1966).

[22] A. J. Strauss, Phys. Rev. **157**, 608 (1967).

[23] T. C. Harman, A. R. Calawa, I. Melngailis, and J. O. Dimmock, Appl. Phys. Lett. **14**, 333 (1969).

[24] A. Svane, N. E. Christensen, M. Cardona, A. N. Chantis, M. van Schilfgaarde, and T. Kotani, Phys. Rev. B **81**, 245120 (2010).

[25] G. Martinez, Phys. Rev. B **8**, 4693 (1973).

[26] B. A. Akimov, R. S. Vadkhva, and S. M. Chudinov, Sov. Phys. Semicond. **12**, 1146 (1978).

[27] P. Blaha, K. Schwarz, G. K. H. Madsen, D. Kvasnicka, and J. Luitz, *WIEN2K, An Augmented Plane Wave + Local Orbitals Program for Calculating Crystal Properties* (Technische Universität Wien, Vienna, Austria, 2001).

[28] S. V. Ovsyannikov, V. V. Shchennikov, A. Y. Manakov, A. Y. Likhacheva, I. F. Berger, A. I. Ancharov, and M. A. Sheromov, Phys. Status Solidi B **244**, 279 (2007).

[29] See Supplemental Material at http://link.aps.org/ supplemental/10.1103/PhysRevLett.113.096401 for details of the structural phase transition, derivation of the Drude weight (including Refs. [30,31]), density of states, parameters from the fitting of reflectance, data for PbTe, and additional band structure data.

[30] C. Ambrosch-Draxl and J. O. Sofo, Comput. Phys. Commun. **175**, 1 (2006).

[31] N. W. Ashcroft and N. D. Mermin, *Solid State Physics* (Holt, Rinehart and Winston, New York, 1976), Appendix E.

[32] P. Y. Yu and M. Cardona, *Fundamentals of Semiconductors* (Springer, New York, 2010), p. 306.

[33] H. Preier, Appl. Phys. **20**, 189 (1979).

[34] Raw data in Fig. 2(a) below 2.0 GPa and in Figs. 3(a) and 3(b) contain interference fringes due to the multiple reflections of the infrared beam in the sample and pressure-transmitting medium. For clarity, these fringes are removed by Fourier transforming the spectra and filtering the associated peaks.

[35] The spectral features for absorbance greater than 2.2 are likely artifacts due to stray light leakage, but they do not affect the analysis discussed here.

[36] X. G. He, X. Xi, and W. Ku (unpublished).

[37] P. Di Pietro, F. M. Vitucci, D. Nicoletti, L. Baldassarre, P. Calvani, R. Cava, Y. S. Hor, U. Schade, and S. Lupi, Phys. Rev. B **86**, 045439 (2012).

[38] A. Akrap, M. Tran, A. Ubaldini, J. Teyssier, E. Giannini, D. van der Marel, P. Lerch, and C. C. Homes, Phys. Rev. B **86**, 235207 (2012).

[39] D. VanGennep, S. Maiti, D. Graf, S. W. Tozer, C. Martin, H. Berger, D. L. Maslov, and J. J. Hamlin, J. Phys. Condens. Matter **26**, 342202 (2014).